

## Marked differences in the $3p$ photoabsorption between the Cr and $\text{Mn}^+$ isoelectronic pair: Reasons for the unique structure observed in Cr

J. W. Cooper, C. W. Clark, C. L. Cromer, and T. B. Lucatorto  
National Bureau of Standards, Gaithersburg, Maryland 20899

B. F. Sonntag

*II. Institute of Experimental Physik, Universität Hamburg, D-2000 Hamburg 50, Federal Republic of Germany*

E. T. Kennedy and J. T. Costello

*School of Physical Sciences, National Institute for Higher Education, Glasnevin, Dublin 9, Ireland*  
(Received 9 February 1989)

Chromium is the only member of the transition-group elements with a well-developed Rydberg structure appearing in its  $3p$ -absorption spectrum. New high-resolution measurements of Mn,  $\text{Mn}^+$ , and Cr have revealed weak Rydberg structure in  $\text{Mn}^+$  and an analysis of the data shows that the anomalous Cr  $3p$  absorption spectra is due to a unique relationship between its energy levels, and not to the previously supposed fact that Cr has an unpaired  $4s$  electron.

For several years now, theorists have been concerned with the question of why Cr was the only member of the iron-group elements that had been studied<sup>1</sup> which has a  $3p$ -photoabsorption spectrum with a set of well-developed Rydberg series. Since Cr is the only member of the iron group with a ground state having an unfilled  $4s$  subshell (and thus an unpaired  $4s$  electron), many thought that the existence of the set of Rydberg series was related to the fact that the lack of the second  $4s$  electron made the Rydberg absorptions sharp by strongly inhibiting the Auger decay from the Rydberg levels (and thus increasing the lifetime). The argument is quite simple. The lowest-lying Rydberg levels are those belonging to series with the highest value of  $S$ , total spin [e.g., for Cr,  $3p^5(3d^5^6S)^7P\ 4s^8P\ ns$  and  $nd$  series; and for Mn,  $3p^5(3d^5^6S)^7P4s^2\ 7P\ ns$  and  $nd$  series]. In these states of Cr, the spin of the  $4s$  electron and the spin of the  $3p$  hole are parallel so that Auger decay involving the filling of the  $3p$  hole by the  $4s$  electron is spin forbidden.

One way of testing the explanation based on Cr's unpaired  $4s$  electron is to observe the  $3p$  photoabsorption of  $\text{Mn}^+$ , Cr's isoelectronic twin having an identical ground-state configuration:  $^1S_0(3d^5^6S)4s^7S_3$ . Our laboratory has the unique capability of observing vacuum ultraviolet (vuv) photoabsorption spectra of relatively cool, homogeneous, dense columns of singly ionized atoms, and we have applied it to the study of  $\text{Mn}^+$ . Preliminary results on  $\text{Mn}^+$  describing changes in the giant  $3p \rightarrow 3d$  resonance structure between Mn and  $\text{Mn}^+$  have been published earlier,<sup>2</sup> but that work lacked the resolution to rule out the existence of  $\text{Mn}^+$  Rydberg levels comparable to those observed in Cr. The present results are definitive:  $\text{Mn}^+$  is qualitatively similar to Mn and the other iron-group atoms—Cr is unique, but for reasons not related to its unpaired  $4s$  electron.

Figure 1 shows the  $3p$  photoabsorption of Mn and  $\text{Mn}^+$  between 47 and 67 eV at three times the resolution of the earlier results.<sup>2</sup> Also shown on Fig. 1 as a comparison is

the  $3p$ -photoabsorption spectra of Cr taken under identical instrumental conditions. The new  $\text{Mn}^+$  spectrum shows some previously unobserved Rydberg structure between 59 and 65 eV, but these are obviously similar to the structures observed in Mn and not at all to Cr. Positions and tentative classification of the resonances observed in  $\text{Mn}^+$  are shown in Table I.

The vuv source used here was a plasma produced by a Nd-doped yttrium aluminum garnet (YAG) laser ( $\approx 0.4$  J, 10–15-nsec pulse width) focused on a tantalum target. The continuum radiation passed through a column of

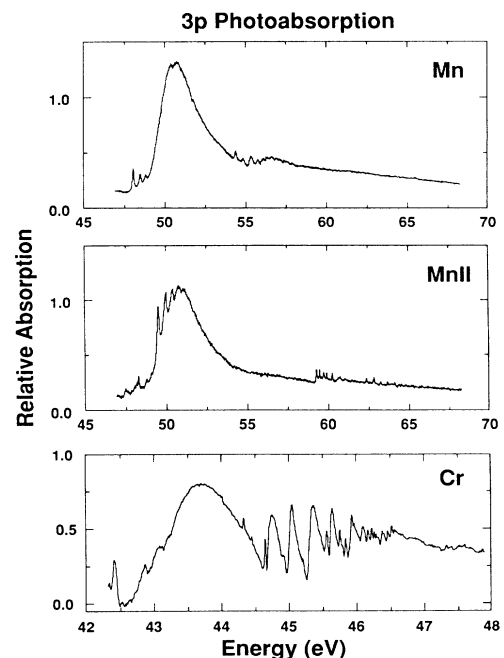


FIG. 1. Relative absorption cross sections for (a) manganese, (b) singly ionized manganese, and (c) chromium.

TABLE I. Resonances in  $Mn^+$   $3p$  subshell absorption. Estimated uncertainty in line positions is  $\pm 0.04$  eV.

Line No.	Energy (eV)	Tentative classification
1	47.50	$3d^6 4s^7 F, ^5 F, ^7 D?$
2	48.20	$3d^6 4s^7 F, ^5 F, ^7 D?$
3	48.30	$3d^6 4s^7 F, ^5 F, ^7 D?$
4	48.80	$3d^6 4s^7 F, ^5 F, ^7 D?$
5	49.11	$3d^6 4s^7 F, ^5 F, ^7 D?$
6	49.53	$3d^5 4s^2 ^7 P_4$
7	50.02	$3d^5 4s^2 ^7 P_3$
8	50.43	$3d^5 4s^2 ^7 P_2$
9	50.81	$3d^6 4s^7 P_{2,3,4}$
10	51.11	$3d^6 4s^7 P_{2,3,4}$
11	59.30	$3d^5 4s 5s ^9 P_4$
12	59.32	
13	59.51	$3d^5 4s 5s ^7 P_4$
14	59.76	$3d^5 4s 5s ^9 P_3$
15	59.94	$3d^5 4s 5s ^7 P_3$
16	60.28	$3d^5 4s 5s ^7 P_2$
17	60.70	$3d^5 4s 4d?$
18	61.09	
19	62.41	
20	62.86	
21	63.28	
22	63.70	
23	64.15	

manganese or chromium vapor approximately 7 cm long confined in a heat-pipe oven by an argon buffer gas. Radiation was focused by a toroidal mirror on the entrance slit of a 1.5-m spectrometer and detection was via an image intensifier and self-scanning diode array. The measured resolution was 0.03 eV.  $Mn^+$  spectra were obtained by exciting the vapor via a coaxial flashlamp-pumped dye laser of 0.5- $\mu$ sec pulse width accurately tuned to the  $^6S$ - $^8P$  transition of Mn at 543.2 nm and taking spectra approximately 1.5  $\mu$ sec after excitation, at which time most of the atoms in the vapor column were ionized. Typically, 200 shots of the YAG laser were made in about 100 sec over the  $\approx 5$ -eV range of the diode array and the furnace was then cooled down to 1200°C to obtain an estimate of the vuv flux as attenuated by the buffer gas. Results for overlapping spectral ranges were matched to obtain rela-

tive transmission data over the entire spectral range covered and relative cross sections were determined using the vuv flux data. Finally, the data were smoothed and the wavelength scale was calibrated using the positions of Al lines produced by using an Al target as the vuv source.

Previous theoretical work<sup>3,4</sup> has provided a basic understanding of the neutral Mn spectra. The main resonance is attributed to three spin-orbit split components of the  $3p^5 3d^6 4s^2$  configuration ( $^6P, J = \frac{3}{2}, \frac{5}{2}, \frac{7}{2}$ ) which are strongly excited and can decay via Coster-Kronig transitions to the  $3d^4 4s^2 \epsilon f$  continuum. Weak structure below the main resonance and above it are attributed to other states of the  $3p^5 3d^6 4s^2$  configuration and to Rydberg states converging to the  $3p^5 3d^5 4s^2$  limits of  $Mn^+$ , respectively. Both Refs. 3 and 4 show that the  $^6P$  resonances lie about 2.2 eV lower than predicted by Hartree-Fock calculations. The Cr spectrum has been analyzed in detail in Ref. 1 and the detailed structure shown in Fig. 1(c) has been attributed to Rydberg series converging to the  $^8P (J = \frac{9}{2}, \frac{7}{2}, \frac{5}{2})$  limits of  $Cr^+ (3p^5 3d^5 4s)$ .

According to the analysis of Ref. 3 the overall shape of the  $^6P$  resonance in Mn can be parametrized via a decay width  $\Gamma$ , an asymmetry parameter  $q$ , and an energy shift due to the strong interaction of the broad resonance with the continuum. We have performed similar calculations<sup>5</sup> for Mn, and for the analogous  $^7P$  resonance in  $Mn^+$ . For Mn our results are similar to those of Ref. 3, the major difference being a smaller half-width (1.37 eV) and a larger  $q$  parameter (2.27) than those of Ref. 3. These values agree well with values obtained via a fit of the experimental data of Ref. 2.<sup>6</sup> For  $Mn^+$  we obtain a half-width of 1.52 eV, a  $q$  value of 2.3, and a somewhat larger energy shift (2.62 eV) which differs only slightly from those of Ref. 3. These theoretical results indicate that there should be little difference in the main resonance peak between Mn and  $Mn^+$ .

As reported in Ref. 2, the interpretation of the three peaks in the 49.5–50.5-eV range are components of a  $3p^5 3d^5 4s^2$  resonance. Our calculations of the positions, strengths, and widths of these resonances for decay to the  $3p^6 3d^4 s \epsilon f$  confirm that analysis. The results are shown in Table II. In order to account for the width of these resonances we have performed configuration interaction calculations between the  $3p^5 3d^6 4s$  and  $3p^5 3d^5 4s^2$  configurations but have shifted the center of gravity of the first

TABLE II. Energies, oscillator strengths, and full widths at half maximum for the  $3p^5 3d^6 4s$  and  $3p^5 3d^5 4s^2 ^7P$  resonances in  $Mn^+$  showing the effects of configuration mixing on the  $3p^5 3d^5 4s^2$  resonances.

State	With configuration mixing			Unmixed, no energy shift		
	Energy (eV)	$f$	$\Gamma$ (eV)	Energy (eV)	$f$	$\Gamma$ (eV)
$3d^5 4s^2 ^7 P_4$	49.33	0.128	0.115	49.35	0.08	0.008
$3d^5 4s^2 ^7 P_3$	49.82	0.135	0.201	49.86	0.07	0.008
$3d^5 4s^2 ^7 P_2$	50.18	0.065	0.373	50.25	0.05	0.008
$3d^6 4s ^7 P_2$	51.28	0.408	2.67	53.83	0.521	
$3d^6 4s ^7 P_3$	51.41	0.642	2.84	53.99	0.738	
$3d^6 4s ^7 P_4$	51.61	0.866	2.93	54.20	0.959	

configuration by 2.62 eV to account for the strong continuum interaction. The results, also shown in Table II, show that there is little shift in energy positions, but a marked increase in widths and oscillator strengths. The increase in widths and decrease in oscillator strengths with decreasing  $J$  values is consistent with the experimental results.

It is not possible to make a definite assignment of the three lowest lying resonances shown in Table I. Although the calculations predict that the  ${}^7F$ ,  ${}^5F$ , and  ${}^7D$  states of the  $3p^5 3d^6 4s$  configuration lie below the  ${}^7P$  states of the  $3p^5 3d^5 4s^2$  configuration, they also indicate that transitions to the  ${}^7F$  states would be too weak to be observed.

Figure 1 shows that there is a marked difference in the structure above the giant resonance peak in Mn, Cr, and  $\text{Mn}^+$ . Previous work<sup>3,4</sup> has indicated that this structure in Mn and Cr is due to  $3p$ - $ns$ ,  $nd$  transitions, but provides little information on the relative positions and strengths of these Rydberg resonances. The present work provides an explanation of these differences.

In strict LS coupling the only allowed transitions will be  ${}^6S_{5/2}$ - ${}^6P_{7/2,5/2,3/2}$  in Mn and  ${}^7S_3$ - ${}^7P_{4,3,2}$  in  $\text{Mn}^+$  and Cr. If we assume that  $3d$  and  $4s$  electrons do not change their coupling when transitions occur, Rydberg states can be considered as  $ns$  and  $nd$  electrons bound to  $3p^5 3d^5 4s^2$ ,  ${}^7P$  cores in Mn and to  $3p^5 3d^5 4s^2$ ,  ${}^6P$  cores in  $\text{Mn}^+$  and Cr. Our identification of the  $3p^5 3d^5 4s^2$  resonances in  $\text{Mn}^+$  determines the  ${}^7P_{4,3,2}$  limits for Rydberg states in Mn, which are in good agreement with those obtained via photoelectron spectroscopy.<sup>7</sup>

The  ${}^8P$  limits in Cr have been determined in Ref. 1 and were found to lie 2.6 eV higher than previous Hartree-Fock estimates.<sup>8</sup> Our calculations, which include an estimate of correlation effects predict these limits to be about 1.3 eV lower than the experimental values. The calculations also show that the analogous  ${}^7P$  limits in Mn lie about 1.2 eV lower than our measurements as shown in Table III. The lowest  ${}^5P$  and  ${}^6P$  limits in each case were found to lie about 2 eV higher than the  ${}^7P$  and  ${}^8P$  limits.

We have also made calculations of the positions and strengths of the lowest  $5s$  resonances in Mn, Cr, and  $\text{Mn}^+$ . The results, shown in Table IV provide a classification of the lowest lying resonances in each case and indicate a partial breakdown of LS coupling. Note that

TABLE III. Series limits for Rydberg resonances in Cr, Mn, and  $\text{Mn}^+$  (in eV above the ground state).

Limit	Calc.	Expt.	Diff.
Cr ${}^8P_{9/2}$	45.05	46.37	1.32
${}^8P_{7/2}$	45.45	46.73	1.28
${}^8P_{5/2}$	45.76	47.05	1.29
Mn ${}^7P_4$	55.71	56.96	1.25
${}^7P_3$	56.20	57.45	1.25
${}^7P_2$	56.55	57.86	1.31
$\text{Mn}^+$ ${}^8P_{9/2}$	64.90		
${}^8P_{7/2}$	65.39		
${}^8P_{5/2}$	65.79		

TABLE IV. Calculated energy levels and oscillator strengths (OS) for  $5s$  states in Mn, Cr, and  $\text{Mn}^+$  reached by  $3p$  excitation.

State	Energy (calc.)	Energy (expt.)	Difference	OS
Mn ${}^6P_{7/2}$	53.40	54.38	0.98	0.0033
${}^8P_{7/2}$	53.78	...		0.0001
${}^6P_{5/2}$	53.91	54.84	0.93	0.0024
${}^8P_{5/2}$	54.18			0.0002
${}^6P_{3/2}$	54.30	55.35	1.05	0.0019
Cr ${}^7P_4$	42.79	44.09 <sup>a</sup>	1.30	0.0019
${}^9P_4$	42.93	44.24 <sup>a</sup>	1.31	0.0008
${}^9P_3$	43.25	44.44 <sup>a</sup>	1.19	0.0008
${}^7P_3$	43.28	44.57 <sup>a</sup>	1.29	0.0013
${}^7P_2$	43.52	44.79 <sup>a</sup>	1.27	0.0015
$\text{Mn}^+$ ${}^9P_4$	58.23	59.31	1.08	0.0022
${}^7P_4$	58.43	59.51	1.08	0.0052
${}^9P_3$	58.64	59.76	1.12	0.0010
${}^7P_3$	58.91	59.94	1.03	0.0050
${}^7P_2$	59.29	60.28	0.99	0.0044

<sup>a</sup>From Ref. 1.

transitions to the five lowest optically allowed  $P$  states are observed in both  $\text{Mn}^+$  and Cr, but that only  ${}^6P$  states are observed in Mn and that the calculated level positions lie below the experimental values by approximately the same values as the series limits shown in Table III.

The resonant structure in  $\text{Mn}^+$  in the 59–65-eV region is shown in more detail in Fig. 2 which points out the similarities and differences between the  $\text{Mn}^+$  and Cr spectra. In  $\text{Mn}^+$  the five lowest  $5s$  resonances lie just below two or possibly three broad resonances which have approximately the same spacing (0.3 eV) as the three broad strong resonances in Cr in the 44.8–45.8 range which were attributed in Ref. 1 to the three lowest lying  $4d$  states.

Thus, the relative positions of the lowest states corresponding to  $5s$  and  $4d$  Rydberg states are similar, the ma-

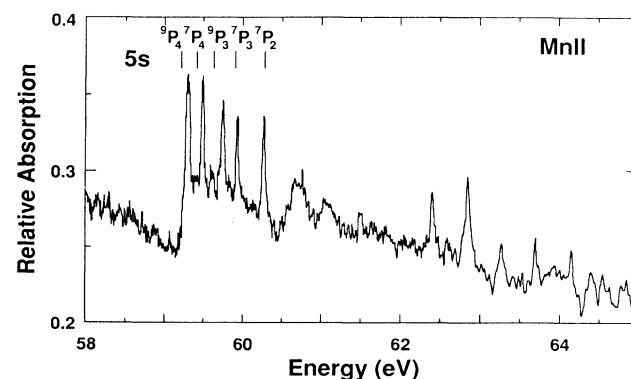


FIG. 2. Resonant structure of ionized manganese in the 59.65-eV range with classifications of the lowest  $5s$  resonances.

major difference being that transitions to  $4d$  states in Cr are much stronger than in  $\text{Mn}^+$ . In order to understand this difference, calculations similar to those reported above for  $5s$  states were also done for the lowest  $4d$  states in Cr and  $\text{Mn}^+$ . These results indicate that the  $4d$  states lie just above the  $5s$  states discussed above, but transitions to these states are somewhat weaker than those to the  $5s$  states. Moreover, the calculated energies of the  $4d$  states do not match the experimental values as they do for the  $5s$  states.

The explanation of these differences is the following. In Cr the  $4d$  states lie only a few eV above the giant  $3d^6 4s^7 P$  giant resonance, whereas in  $\text{Mn}^+$  the relative spacing is about 8 eV. Due to the close proximity, we expect strong mixing between the  $3d^6 4s^7 P$  resonance in Cr and Rydberg states belonging to  $3d^5 4s nd$  configurations resulting in a transfer of oscillator strength to  $nd$  Rydberg states, but relatively little mixing for the similar case in  $\text{Mn}^+$ .

While a detailed calculation of these complex spectra will require further theoretical work, preliminary calcula-

tions indicate that the analysis given above is substantially correct. We find that mixing between the  $3d^6 4s$  and  $3d^5 4s 4d$  configurations is stronger than that between  $3d^6 4s$  and  $3d^5 4s 5s$  in both Cr and  $\text{Mn}^+$ . Our calculations ignoring configuration mixing also predict that the  $^7P$  giant resonance in Cr lies above the  $\text{Cr}^+ \ ^8P$  limits in agreement with previous results,<sup>8</sup> and has a width comparable to that of the Mn and  $\text{Mn}^+$  resonances. These results imply that a realistic calculation of the Cr spectra must include configuration mixing of the  $3d^6 4s^7 P$  resonance with continuum states as well as with the  $3d^5 4s nd$  configurations.

In summary, our results provide for the first time a definitive study of the  $3p$  subshell giant resonance in  $\text{Mn}^+$  and offer an explanation of the marked differences between the resonance structure in  $\text{Mn}^+$  and Cr.

We would like to acknowledge partial support by the Air Force Office of Scientific Research under Contract No. ISSA-87-0050 and important technical assistance from Dr. Frank Tomkins and Dr. Junwen Cui.

<sup>1</sup>R. Bruhn, E. Schmidt, H. Schröder, and B. F. Sonntag, *J. Phys. B* **15**, 2807 (1982); M. Meyer, Th. Prescher, E. von Raven, M. Richter, E. Schmidt, B. F. Sonntag, and H. E. Wetzel, *Z. Phys. D* **2**, 347 (1986).

<sup>2</sup>J. W. Cooper, C. W. Clark, C. L. Cromer, T. B. Lucatorto, B. F. Sonntag, and F. S. Tomkins, *Phys. Rev. A* **35**, 3970 (1987).

<sup>3</sup>L. C. Davis and L. H. Feldkamp, *Phys. Rev. A* **17**, 2012 (1978).

<sup>4</sup>L. J. Garvin, I. R. Brown, S. L. Carter, and H. P. Kelly, *J. Phys. B* **16**, L269 (1983).

<sup>5</sup>The calculations were done using programs developed by R. Cowan. See R. Cowan, *The Theory of Atomic Structure and Spectra* (Univ. California Press, Berkeley, 1981) for a description of the methods used.

<sup>6</sup>H. Koberle, DESY Report No. F41, Hasylab 8603, 1986 (unpublished).

<sup>7</sup>R. Malutzki, M. S. Banna, W. Braun, and V. Schmidt, *J. Phys. B* **18**, 1735 (1985).

<sup>8</sup>M. W. D. Mansfield, *Proc. R. Soc. London, Ser. A* **358**, 253 (1977).